



Title	Probing the coupled adhesion and deformation characteristics of suspension cells
Author(s)	Hui, TH; Zhu, Q; Zhou, ZL; Qian, J; Lin, Y
Citation	Applied Physics Letters, 2014, v. 105 n. 7, article no. 073703, p. 073703:1-5
Issued Date	2014
URL	http://hdl.handle.net/10722/203035
Rights	Applied Physics Letters. Copyright © American Institute of Physics.



Probing the coupled adhesion and deformation characteristics of suspension cells

T. H. Hui, Q. Zhu, Z. L. Zhou, J. Qian, and Y. Lin

Citation: [Applied Physics Letters](#) **105**, 073703 (2014); doi: 10.1063/1.4893734

View online: <http://dx.doi.org/10.1063/1.4893734>

View Table of Contents: <http://scitation.aip.org/content/aip/journal/apl/105/7?ver=pdfcov>

Published by the [AIP Publishing](#)

Articles you may be interested in

[Total three-dimensional imaging of phase objects using defocusing microscopy: Application to red blood cells](#)
Appl. Phys. Lett. **104**, 251107 (2014); 10.1063/1.4884420

[Single-cell adhesion probed in-situ using optical tweezers: A case study with *Saccharomyces cerevisiae*](#)
J. Appl. Phys. **111**, 114701 (2012); 10.1063/1.4723566


[Method for measuring the three-dimensional distribution of a fluorescent dye in a cell membrane](#)
Appl. Phys. Lett. **90**, 021110 (2007); 10.1063/1.2428457

[Machine vision and feedback control system allow the precise control of vascular deformation in vitro](#)
Rev. Sci. Instrum. **77**, 064304 (2006); 10.1063/1.2216872

[Three-dimensional numerical simulation of receptor-mediated leukocyte adhesion to surfaces: Effects of cell deformability and viscoelasticity](#)
Phys. Fluids **17**, 031505 (2005); 10.1063/1.1862635

The logo for Applied Physics Letters (AIP) is displayed in white text on an orange background. The background features a pattern of vertical, wavy lines that resemble light reflecting off a liquid surface.

Meet The New Deputy Editors

	Alexander A. Balandin		Qing Hu		David L. Price
---	-----------------------	---	---------	--	----------------

Probing the coupled adhesion and deformation characteristics of suspension cells

T. H. Hui,¹ Q. Zhu,¹ Z. L. Zhou,¹ J. Qian,^{2,a)} and Y. Lin^{1,a)}

¹Department of Mechanical Engineering, The University of Hong Kong, Hong Kong, China

²Department of Engineering Mechanics, Zhejiang University, Hangzhou, Zhejiang, China

(Received 5 May 2014; accepted 11 August 2014; published online 20 August 2014)

By combining optical trapping with fluorescence imaging, the adhesion and deformation characteristics of suspension cells were probed on single cell level. We found that, after 24 h of co-culturing, stable attachment between non-adherent K562 cells and polystyrene beads coated with fibronectin, collagen I, or G-actin can all be formed with an adhesion energy density in the range of $1\text{--}3 \times 10^{-2}$ mJ/m², which is about one order of magnitude lower than the reported values for several adherent cells. In addition, it was observed that the formation of a stronger adhesion is accompanied with the appearance of a denser actin cell cortex, especially in the region close to the cell-bead interface, resulting in a significant increase in the apparent modulus of the cell. Findings here could be important for our understanding of why the aggregation of circulating cells, like that in leukostasis, takes place *in vivo* as well as how such clusters of non-adherent cells behave. The method proposed can also be useful in investigating adhesion and related phenomena for other cell types in the future. © 2014 AIP Publishing LLC. [<http://dx.doi.org/10.1063/1.4893734>]

Adhesion plays important roles in processes such as cell migration,¹ differentiation,² proliferation,³ and cell death.⁴ For this reason, intense effort has been spent to characterize the interactions between living cells and their micro-environment. In particular, techniques like atomic force microscopy (AFM),⁵ interference microscopy,⁶ micropipette manipulation,⁷ laser spallation,⁸ and shear flow assay⁹ have all been developed to probe cell-substrate or cell-cell adhesion. A common theme of these approaches is to induce cell detachment from the substrate (or other cells) with imposed disruptive “forces” (e.g., laser shock, shear flow, and direct pulling) from which the adhesion characteristics can be quantitatively extracted. However, due to the non-trivial geometry and deformability of cells, proper theoretical models are often needed to interpret data from such experiments. One popular choice to serve this purpose is the Johnson-Kendall-Roberts (JKR) theory¹⁰ where the effect of adhesion is represented by a single parameter (adhesion energy density) and relationships describing the spontaneous attachment as well as enforced separation of two elastic spheres have all been obtained in simple forms. Actually, in addition to being used to analyze cellular attachment,⁷ the JKR approach has also been adopted in examining biological adhesion of vesicles,¹¹ nanoparticles,¹² and objects with wavy surfaces.^{13,14}

Despite these aforementioned efforts, several important issues remain to be further explored. For one thing, most existing experiments focus on adherent cells but very little has been reported regarding the adhesion response of suspension cells. Of course, by their nature, non-adherent cells usually cannot establish strong attachment with the outside. Nevertheless, under pathological conditions such as leukostasis circulating leukocytes can form aggregates, obstruct small vessels in organs, and eventually lead to serious problems like convulsion, stroke, visual, and auditory

impairment.^{15–17} Evidently, a precise knowledge of the adhesion characteristics of these non-adherent cells will be important for our understanding of how such phenomenon takes place as well as for finding possible prevention/treatment strategies. In addition, although it is widely known that the formation of tight contact regions (often referred to as focal adhesions) between cells and the extracellular matrices (ECMs) requires the assembly of numerous proteins in the intracellular side,¹ very few studies have explored the question of whether and how the appearance of adhesion alters the mechanical response of cells.

Aiming to address these issues, we developed a method to quantitatively measure the adhesion response of individual suspension cells by combined optical trap manipulation and fluorescence. Specifically, precisely controlled optical pulling was applied to ligand-coated polystyrene beads that are in adhesive contact with K562 (human chronic myelogenous leukemia) cells. Evolutions of the contact area and bead movement during the detaching process were recorded which, in conjunction with the JKR description, allow us to extract the adhesion energy density of the cell-bead interface as well as the cell modulus. Fluorescence imaging was also utilized to monitor possible adhesion-induced cytoskeletal changes.

Fibronectin and collagen I, two common adhesion proteins, are known to be important for the immobilization of living cells within tissues and organs,^{18,19} as well as facilitate cell-substrate adhesion *in vitro*.^{20,21} In addition, it is conceivable that attachment of cells to the surface deposited with actin, a molecule heavily involved in the formation of focal adhesions²² and capable of binding to various membrane-associated proteins and receptors,²³ can take place. Based on these observations, we focus our attention on the adhesion between suspension K562 cells and beads coated with the three aforementioned ligands, respectively. Specifically, cells were co-cultured with 5 μm-polystyrene beads (Polysciences), deposited with fibronectin (Sigma), actin (Molecular Probes) or collagen I (Sigma), on a fibronectin-coated confocal dish

^{a)}Authors to whom correspondence should be addressed. Electronic addresses: jqian@zju.edu.cn and ylin@hku.hk.

for 24 h, see supplementary material²⁴ for details. After that, optical trap (MMI) was used to grab individual microspheres, in adhesive contact with K562 cells, and then pull them away from the cells immobilized on the cover-slip as illustrated in Fig. 1(a). Videos were taken during the entire separation process to record the bead displacement in time, $u(t)$, as well as changes in the contact radius a . Since the motion of the laser, i.e., $\delta(t)$ as shown in Fig. 1(a), is controlled in our experiment, the quantity $\delta - u$ represents the relative displacement between the bead and the laser beam which, in return, leads to a trapping potential on the bead tending to minimize $|\delta - u|$.

It has been shown that optical trap works approximately like a linear spring,^{25,26} so that a force

$$F(t) = -k[\delta(t) - u(t)] \quad (1)$$

will be exerted on the microsphere confined within the laser beam with the negative sign representing that this force is

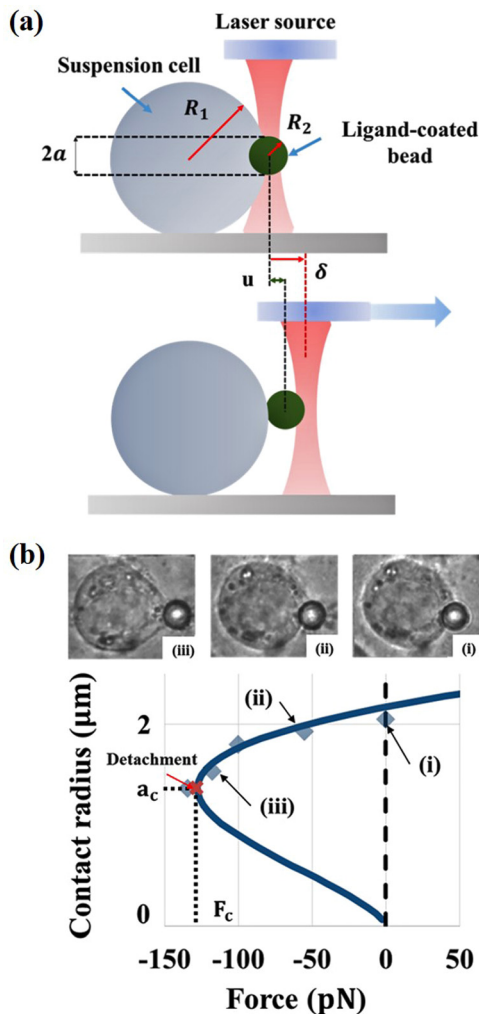


FIG. 1. (a) Schematic diagram of a K562 cell (with radius R_1) in adhesive contact with a microsphere (with radius R_2), where the contact radius is denoted as a . A laser beam is used to trap the bead and then pull it away from the cell, with δ and u representing the displacement of the laser (controlled) and the bead, respectively. (b) Typical force versus contact radius relationship obtained from our test. Micrographs of a deformed cell during the pulling process are provided in the insets. The solid line illustrates the predictions from the JKR theory with F_c and a_c being the so-called pull off force and the corresponding critical contact radius.

“tensile,” i.e., trying to separate the bead from the cell. Here, k is the effective stiffness of the trap whose value depends on factors like the laser power and bead size and hence must be calibrated beforehand, see supplementary material²⁴ for the calibration protocol. In this study, a constant trapping stiffness of $39.7 \text{ pN}/\mu\text{m}$ was used. With a method of estimating the pulling force at hand, we can then construct the F vs. a curve for the detaching process, as illustrated in Fig. 1(b), which is of key interest in the study of adhesive contact. To make sure changes in the contact area can be accurately monitored, special attention has been paid to identify microspheres adhering to the side (not to the upper or lower portion) of the cell, based on which all our tests were conducted.

In addition to optical manipulation, immunofluorescent imaging was also employed to monitor possible adhesion-induced cytoskeletal changes in K562 cells. In particular, cells were fixed with 3.7% paraformaldehyde, permeabilized with 0.1% Triton X-100, and then stained against F-actin with AF488-phalloidin (Invitrogen) prior to experiment. After co-culturing with ligand-coated microspheres, a fluorescence microscope (Nikon) was used to obtain images of cells in adhesion.

A representative sequence of micrographs of a K562 cell subjected to optical pulling is shown in Fig. 1(b). As the magnitude of F increases, deformation of the cell becomes more apparent and the contact area keeps shrinking gradually. Finally, detachment between the cell and the bead takes place abruptly after F reaches a critical level. Data from multiple independent tests for each case, i.e., beads coated with fibronectin ($n = 10$), collagen I ($n = 12$), actin ($n = 13$), or without coating ($n = 8$), are gathered in Fig. 2(a). Compared to the case of non-coating beads, the presence of fibronectin or collagen I noticeably elevates the maximum pulling force (from $\sim 90 \text{ pN}$ to $\sim 130 \text{ pN}$) that the adhesion can sustain. Interestingly, coating the bead surface with actin further increases the pull-off force to the range of $\sim 250\text{--}300 \text{ pN}$. Recall that, according to the well-known JKR theory, the enforced separation between two elastic spheres in adhesive contact can be described by²⁷

$$\left[F - \frac{4E_r a^3}{3R} \right]^2 = 8\pi\gamma E_r a^3, \quad (2)$$

where a and F , as defined before, are the contact radius and applied force; γ is the adhesion energy density representing the energy reduction per unit area when two surfaces are brought together; and $1/R = 1/R_1 + 1/R_2$ where R_1 ($\approx 10 \mu\text{m}$) and R_2 ($= 2.5 \mu\text{m}$) are the radii of the cell and the bead (Fig. 1(a)). Since the microsphere is much stiffer than the cell, the so-called reduced cell modulus (E_r) takes the form $E_r = \frac{E_1}{1-\nu_1^2}$, with E_1 and ν_1 (≈ 0.5) being the Young’s modulus and Poisson’s ratio of the cell, respectively.

The generic shape of the F vs. a curve, according to Eq. (2), is schematically shown in Fig. 1(b) by the solid line where the critical pulling force for triggering sudden detachment is predicted to be $F_c = -\frac{2}{3}\gamma\pi R$, with a corresponding contact radius of $a_c = \left[\frac{9R^2\gamma\pi}{8E_r} \right]^{1/3}$. As illustrated in Fig. 2(a), our data can be well explained by Eq. (2) if one chooses $\gamma = 0.03 \text{ mJ}/\text{m}^2$ and $E_r = 100 \text{ Pa}$ for actin coating,

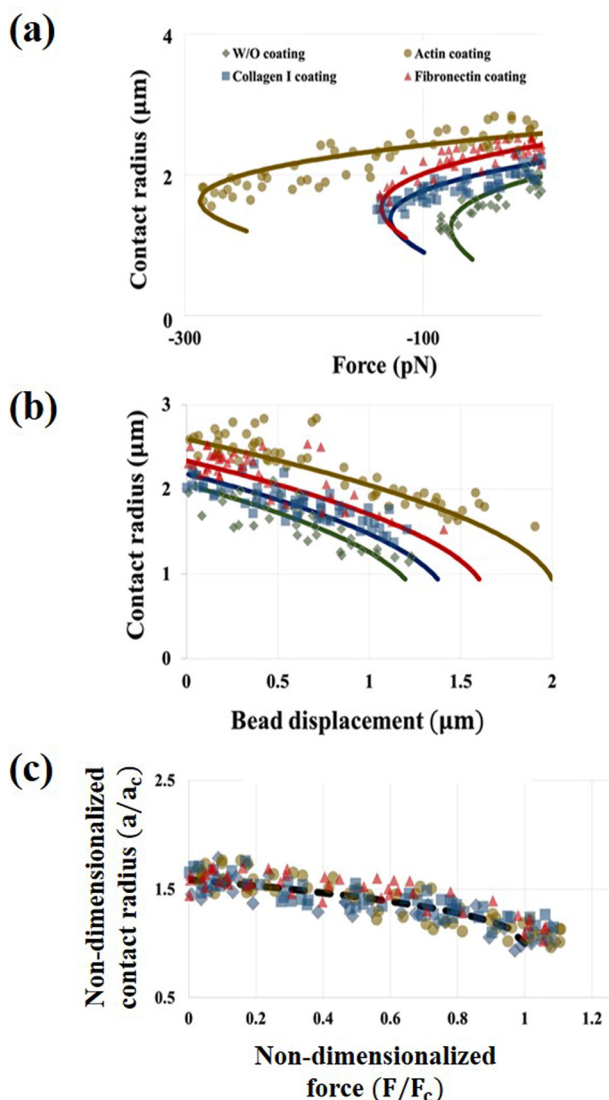


FIG. 2. (a) Contact radius as a function of the pulling force. Markers represent measurement data while solid lines correspond to JKR predictions, i.e., Eq. (2). (b) Relationship between the bead displacement and contact radius where solid lines represent predictions from Eq. (3). (c) Normalized contact radius a/a_c versus normalized pulling force F/F_c with the dashed line corresponding to the relationship given in Eq. (4). Theoretical predictions are obtained by choosing $\gamma = 0.03 \text{ mJ/m}^2$ and $E_r = 100 \text{ Pa}$ for actin coating; $\gamma = 0.0143 \text{ mJ/m}^2$ and $E_r = 71.3 \text{ Pa}$ for fibronectin; $\gamma = 0.0127 \text{ mJ/m}^2$ and $E_r = 75 \text{ Pa}$ for collagen I; and $\gamma = 0.009 \text{ mJ/m}^2$ and $E_r = 60.3 \text{ Pa}$ for no coating. In addition, the least square method was used to achieve the best fitting.

$\gamma = 0.0143 \text{ mJ/m}^2$ and $E_r = 71.3 \text{ Pa}$ for fibronectin, $\gamma = 0.0127 \text{ mJ/m}^2$ and $E_r = 75 \text{ Pa}$ for collagen I, and $\gamma = 0.009 \text{ mJ/m}^2$ and $E_r = 60.3 \text{ Pa}$ for no coating. To avoid possible inaccuracies involved in estimating the trapping force, we can also plot the bead displacement against contact radius, two quantities that were directly measured in our experiment, as illustrated in Fig. 2(b). It can be shown that, within the JKR framework, the relative approach between the cell and the bead equals to $\sqrt{\frac{\pi\gamma a_0}{2E_r}}$ (where $a_0 = \left[\frac{9R^2\gamma\pi}{2E_r}\right]^{1/3}$ is the initial contact radius) when $F = 0$ but then changes to $\frac{a^2}{R} - \sqrt{\frac{2\pi\gamma a}{E_r}}$ once the applied force becomes non-vanishing. Given that the cell is immobilized on the substrate, u essentially represents the difference between these two quantities, that is

$$u = \sqrt{\frac{\pi\gamma}{2E_r}}(2\sqrt{a} + \sqrt{a_0}) - \frac{a^2}{R}. \quad (3)$$

Adopting the same γ and E_r values as those in Fig. 2(a), predictions from Eq. (3) are shown by the solid lines in Fig. 2(b) which, evidently, are in good agreement with experimental observations. We realize that the best way to visualize the comparison between our results and predictions from the JKR model is to plot F/F_c against a/a_c , with F_c and a_c calculated from the corresponding γ and E_r values for each coating condition. Note that, based on the definitions of F_c and a_c , Eq. (2) can be rewritten in the normalized form as

$$\left(\frac{a}{a_c}\right)^3 = 2 - F/F_c + 2\sqrt{1 - F/F_c}. \quad (4)$$

Indeed, all data collapse into a single master curve in the F/F_c vs. a/a_c plot (Fig. 2(c)), as predicted by Eq. (4), further demonstrating that, irrespective of the types of ligands being used, the adhesion response of these suspension cells can always be well described by the JKR theory.

One thing must be pointed out is that the results obtained from our experiments are rather consistent with each other. For example, by fitting Eq. (2) to data from each pulling test, the bar graphs of extracted γ and E_r are shown in Figs. 3(a) and 3(b) which demonstrate that variation in the values of these two parameters is rather small. Interestingly, results here also suggest that a stronger adhesion is accompanied with a larger cell modulus. In particular, according to Fig. 3(b), K562 cells in contact with actin-coated beads appear to possess a modulus that is $\sim 60\%$ higher than that exhibited by cells adhering to microspheres without coating. To confirm this finding, we have conducted additional AFM rate-jump indentations^{28,29} on K562 cells (20 independent tests for each coating), as detailed in the supplementary material,²⁴ where similar trend was also observed (Fig. 3(b)).

It is conceivable that the formation of adhesion can trigger protein assembly in the cytoskeleton, strengthen the cell body, and eventually lead to an elevated apparent modulus. To test this hypothesis, the density of F-actin, a major cytoskeletal component, in K562 cells was monitored by fluorescence imaging. As expected, compared to the control group (i.e., cells in contact with microspheres without coating), a much denser actin cell cortex, especially in the region close to the cell-bead interface, was observed in cells attaching to actin-coated beads (Fig. 3(c) and Fig. S2 in the supplementary material²⁴). We further quantify these results by calculating the average fluorescent intensity in the 500 nm-thick layer underneath the membrane-bead interface as well as plotting the intensity distribution along the path starting at the center of the interface and moving into the cell, as indicated by the red dashed loop and white dashed arrow in Fig. 3(c). Clearly, results here show that coating the bead with fibronectin or collagen I leads to a $\sim 50\%$ increase in the F-actin intensity while the deposition of G-actin roughly doubles that. These evidences support the notation that the formation of adhesion is coupled with the local reinforcement of F-actin in the cytoskeleton, resulting in a higher resistance of the cell against deformation.

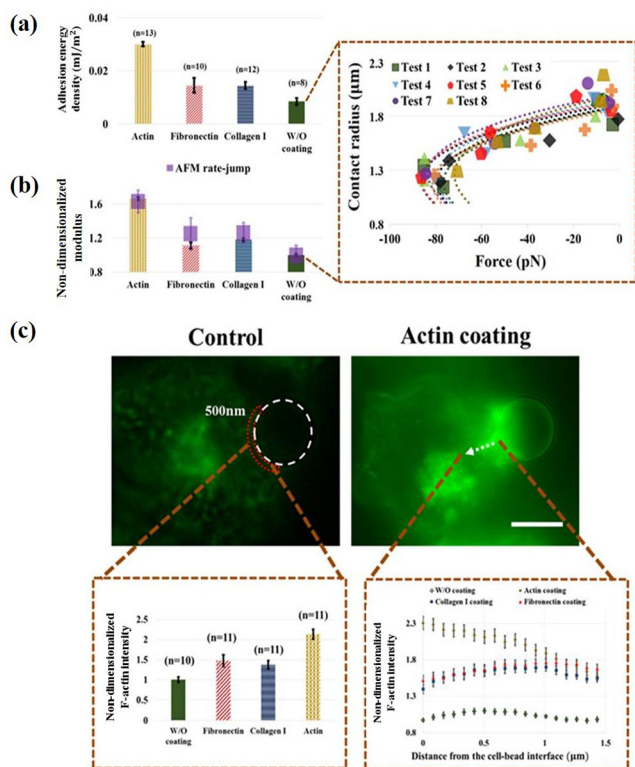


FIG. 3. (a) Bar graph of the adhesion energies extracted by fitting Eq. (2) to data from each test, as illustrated in the inset for the case of no coating, where n is the number of independent pulling experiments being conducted. (b) Bar plot of the extracted reduced moduli of K562 cells where the values have been normalized by the average modulus (60.3 Pa) of cells attaching to beads without coating. Results from AFM rate-jump indentations (see supplementary material²⁴), with 20 independent tests for each coating, are also included here. (c) Immunofluorescent staining of F-actin in K562 cells adhering to microspheres deposited with actin or w/o coating (control) where the scale bar represents 5 μm . Average fluorescent intensities (normalized by the value corresponding to the control group) of cortical F-actin within the 500 nm-thick layer underneath the cell-bead interface (the red dashed loop) are shown in the bottom left. In addition, distributions of F-actin intensity along the path starting at the center of the interface and moving into the cell, indicated by the white dashed arrow, are also plotted in the bottom right. A statistical confidence level of no less than 97% by t-test has been achieved for all the results shown in (a), (b), and (c).

In this study, we have developed a method to quantitatively measure the adhesion and deformation of suspension cells on single cell level. Specifically, we found that adhesion between K562 cells and polystyrene beads coated with (or without) common cell-binding ligands can be formed with an energy reduction in the range of $1\text{--}3 \times 10^{-2}$ mJ/m², a value that is comparable to those found for mutants of *Dictyostelium*⁶ or some pure bilayer systems.³⁰ In comparison, this energy for several adherent cells, including T-lymphocytes³¹ and murine sarcoma S180 cells,⁷ has been reported to be of the order of 10^{-1} mJ/m². The relatively weak adhesion capability of K562 cells is not that surprising given their non-adherent nature, that is, these cells normally do not adhere to each other or to the outside. Nevertheless, it is well-known that conditions such as leukostasis can trigger the aggregation and clumping of circulating blood cells and lead to serious medical issues. As such, data obtained here should help us understand how phenomena like this take place as well as identify possible prevention/treatment strategies. Our results also demonstrated that, compared to

fibronectin or collagen I, coating the surface with G-actin will lead to stronger cell attachment, a finding that surprisingly has hardly been reported. Identification of the molecular mechanism behind is beyond the scope of current study and is certainly an issue that warrants further investigation.

Most existing studies treated the adhesion energy density and cell modulus as *independent* quantities.^{7,12} However, observations here clearly suggest that these two parameters are coupled for the investigated system. In particular, cells adhering to actin-coated beads appear to have a modulus that is significantly ($\sim 60\%$) higher than those bound to microspheres without coating (Fig. 3(b)). This finding could be important in the modeling of adhesion mediated processes, as well as interpreting experimental data, in the future. For example, according to the present study, cell aggregates can become much stiffer than individual cells, a feature that may have great implications in analyzing the deformation³² or migration³³ behavior of cell clusters. The approach proposed here may also be of immediate use in examining issues like how membrane fluctuations^{34,35} or stochastic transitions in protein binding/unbinding^{36,37} affect weak cell-cell or cell-substrate interactions^{38,39} given that forces in the range of piconewton can be precisely applied in the current setup.

This work was supported by a grant from the Research Grants Council (Project No. HKU 7143/12E) of the Hong Kong Special Administration Region as well as a seed fund (Project No. 201211159001) from The University of Hong Kong. J.Q. acknowledges support from the National Natural Science Foundation of China (Nos. 11202184 and 11321202).

- ¹J. T. Parsons, A. R. Horwitz, and M. A. Schwartz, *Nat. Rev. Mol. Cell Biol.* **11**(9), 633–643 (2010).
- ²L. Bacakova, E. Filova, M. Parizek, T. Ruml, and V. Svorcik, *Biotechnol. Adv.* **29**(6), 739–767 (2011).
- ³M. A. Kafi, W. A. El-Said, T. H. Kim, and J. W. Choi, *Biomaterials* **33**(3), 731–739 (2012).
- ⁴D. G. Stupack and D. A. Cheresch, *J. Cell Sci.* **115**(19), 3729–3738 (2002).
- ⁵P. Y. Meadows and G. C. Walker, *Langmuir* **21**(9), 4096–4107 (2005).
- ⁶R. Simson, E. Wallraff, J. Faix, J. Niewohner, G. Gerisch, and E. Sackmann, *Biophys. J.* **74**(1), 514–522 (1998).
- ⁷Y. S. Chu, S. Dufour, J. P. Thiery, E. Perez, and F. Pincet, *Phys. Rev. Lett.* **94**(2), 028102 (2005).
- ⁸E. Hagerman, J. Shim, V. Gupta, and B. Wu, *J. Biomed. Mater. Res., Part A* **82A**(4), 852–860 (2007).
- ⁹Z. Tang, Y. Akiyama, K. Itoga, J. Kobayashi, M. Yamato, and T. Okano, *Biomaterials* **33**(30), 7405–7411 (2012).
- ¹⁰K. L. Johnson, K. Kendall, and A. D. Roberts, *Proc. R. Soc. London* **324**(1558), 301–313 (1971).
- ¹¹Y. Lin and L. B. Freund, *Int. J. Solids Struct.* **44**(6), 1927–1938 (2007).
- ¹²J. Lin, Y. Lin, and J. Qian, *Langmuir* **30**(21), 6089–6094 (2014).
- ¹³P. R. Guduru and C. Bull, *J. Mech. Phys. Solids* **55**(3), 473–488 (2007).
- ¹⁴P. R. Guduru, *J. Mech. Phys. Solids* **55**(3), 445–472 (2007).
- ¹⁵R. Naithani, J. Chandra, N. N. Mathur, S. Narayan, and V. Singh, *Pediatr Blood Cancer* **45**(1), 54–56 (2005).
- ¹⁶D. E. Joseph and M. A. Durosini, *Niger. J. Clin. Pract.* **11**(3), 246–249 (2008).
- ¹⁷M. Gokce, S. Unal, B. Bayrakci, and M. Tuncer, *Indian J. Hematol. Blood Transfus.* **26**(3), 96–98 (2010).
- ¹⁸J. R. Couchman, M. R. Austria, and A. Woods, *J. Invest. Dermatol.* **94**(s6), 7s–14s (1990).
- ¹⁹J. Heino, *Bioessays* **29**(10), 1001–1010 (2007).
- ²⁰K. Aoshiba, S. I. Rennard, and J. R. Spurzem, *Am. J. Physiol.* **273**(3), L684–L693 (1997).

- ²¹J. Jokinen, E. Dadu, P. Nykvist, J. Kapyla, D. J. White, J. Ivaska, P. Vehvilainen, H. Reunanen, H. Larjava, L. Hakkinen, and J. Heino, *J. Biol. Chem.* **279**(30), 31956–31963 (2004).
- ²²B. Geiger, J. P. Spatz, and A. D. Bershadsky, *Nat. Rev. Mol. Cell Biol.* **10**(1), 21–33 (2009).
- ²³C. G. dos Remedios, D. Chhabra, M. Kekic, I. V. Dedova, M. Tsubakihara, D. A. Berry, and N. J. Nosworthy, *Physiol. Rev.* **83**(2), 433–473 (2003).
- ²⁴See supplementary material at <http://dx.doi.org/10.1063/1.4893734> for additional information on bead coating and cell culture; optical tweezers calibration; rate-jump indentation; and fluorescent images of K562 cells in adhesive contact.
- ²⁵Z. L. Zhou, B. Tang, and A. H. W. Ngan, *Nano LIFE* **02**(1), 1250010 (2012).
- ²⁶M. Andersson, A. Madgavkar, M. Stjern Dahl, Y. Wu, W. Tan, R. Duran, S. Niehren, K. Mustafa, K. Arvidson, and A. Wennerberg, *Rev. Sci. Instrum.* **78**, 074302 (2007).
- ²⁷K. L. Johnson, *Contact Mechanics*. (Cambridge University Press, Cambridge, UK, 1987).
- ²⁸A. H. W. Ngan and B. Tang, *J. Mater. Res.* **24**(3), 853–862 (2009).
- ²⁹B. Tang and A. H. W. Ngan, *Soft Matter* **8**(22), 5974–5979 (2012).
- ³⁰D. Boal, *Mechanics of the Cell*. (Cambridge University Press, Cambridge, UK, 2002).
- ³¹I. B. Ivanov, A. Hadjiiski, N. D. Denkov, T. D. Gurkov, P. A. Kralchevsky, and S. Koyasu, *Biophys. J.* **75**(1), 545–556 (1998).
- ³²P. Marmottant, A. Mgharbel, J. Kafer, B. Audren, J. P. Rieu, J. C. Vial, B. van der Sanden, A. F. M. Maree, F. Graner, and H. Delanoe-Ayari, *Proc. Natl. Acad. Sci. U.S.A.* **106**(41), 17271–17275 (2009).
- ³³J. Youssef, A. K. Nurse, L. B. Freund, and J. R. Morgan, *Proc. Natl. Acad. Sci. U.S.A.* **108**(17), 6993–6998 (2011).
- ³⁴Y. Lin, M. Inamdar, and L. B. Freund, *J. Mech. Phys. Solids* **56**(1), 241–250 (2008).
- ³⁵L. B. Freund, *Proc. Natl. Acad. Sci. U.S.A.* **110**(6), 2047–2051 (2013).
- ³⁶J. Qian, Y. Lin, H. Y. Jiang, and H. M. Yao, *Appl. Phys. Lett.* **103**(22), 223702 (2013).
- ³⁷D. C. Li and B. H. Ji, *Phys. Rev. Lett.* **112**(7), 078302 (2014).
- ³⁸Y. Lin and L. B. Freund, *Phys. Rev. E* **78**(2), 021909 (2008).
- ³⁹L. Sun, Q. H. Cheng, H. J. Gao, and Y. W. Zhang, *J. R. Soc. Interface* **9**(70), 928–937 (2012).